Construction and Building Materials 456 (2024) 139309

Contents lists available at ScienceDirect

Construction and Building Materials

journal homepage: www.elsevier.com/locate/conbuildmat

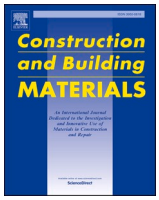

Solar-optical and thermal behavior of photochromic glazing: Small-scale testing under real sky conditions

Henriqueta Teixeira [a,*], A. Moret Rodrigues [a], Daniel Aelenei [b,c], Isabel Ferreira [d], M. Glória Gomes [a]

[a] CERIS, DECivil, IST, Universidade de Lisboa, Av. Rovisco Pais, Lisbon 1049-001, Portugal
[b] UNINOVA-CTS, DEC, FCT, Universidade Nova de Lisboa, Caparica 2829-516, Portugal
[c] LASI, Guimarães 4800-058, Portugal
[d] CENIMAT|I3N, DCM, FCT, Universidade Nova de Lisboa, Caparica 2829-516, Portugal

ARTICLE INFO

Keywords:
Photochromic glazing
Thermal performance
Solar-optical performance
Small-scale
Real sky conditions

ABSTRACT

The poor performance of conventional building glazing, which is usually responsible for large climatization needs and glare problems, has been promoting the development of innovative smart glazing technologies with an improved performance. Photochromic glazing, a type of smart glazing, exhibits a dynamic behavior by darkening/bleaching in reaction to the presence/absence of solar radiation. The aim of this study is to evaluate the thermal and solar-optical behavior of a photochromic filmed clear glazing, against the same glazing without film, through experimental tests. The transmittance and reflectance spectra of the glazing solutions were initially measured with a spectrophotometer. Then two small-scale models were used to assess the behavior of the glazing solutions under real sky conditions (clear and overcast). The thermal behavior was assessed through air and surface temperature measurements. The solar-optical behavior was investigated through solar radiation and illuminance measurements, which were also used to compute the solar and visible transmittance of the glazing systems, respectively. The dynamic behavior of the photochromic film resulted on a reduction of 14 % of the interior temperature. Interior illuminance and irradiance levels were significantly reduced with the film, corresponding to 10–50 % and 15–35 % visible and solar transmittance values of the photochromic glazing, respectively.

1. Introduction

Glazing systems of façades significantly influence the thermal and luminous performance of buildings, consequently affecting their energy performance [1,2]. Conventional glazing systems, which are usually passive, are limited by atmospheric conditions, often requiring artificial lighting and/or climatization equipment to ensure adequate visual and/or thermal indoor comfort conditions.

To mitigate these limitations, solar control coating layers [3] can be applied during the glazing manufacturing process, or alternatively, solar control films [4] can be retrofitted onto existing glazing to improve performance. There are different types of solar control coatings and films available on the market that can be classified as neutral, reflective, dual-reflective, low-emissivity or spectrally selective. These solar control coatings and films promote energy savings and indoor visual and thermal comfort conditions [5–7], particularly in hot climates with higher solar radiation levels, providing a better performance than uncoated glazing. While effective, these static solutions lack the ability to adapt to dynamic environmental conditions or occupant needs, which may reduce their effectiveness in highly variable climates.

The rise of highly glazed buildings, promoted by current architectural trends, coupled with the ambition of promoting sustainable buildings with a high energy performance [8], has driven the investigation and development of innovative glazing technologies. Among these innovative technologies are smart glazing systems that react to specific stimuli (such as temperature, solar radiation, electric power), altering their thermal and optical properties and, consequently, adapting to surrounding environmental conditions and combining multiple performance requirements [9,10]. This dynamic behavior aims at reducing cooling energy needs in the presence of high solar radiation

* Correspondence to: Av. Rovisco Pais, Lisbon 1049-001, Portugal.
E-mail addresses: henriqueta.teixeira@tecnico.ulisboa.pt (H. Teixeira), moret.rodrigues@tecnico.ulisboa.pt (A. Moret Rodrigues), aelenei@fct.unl.pt (D. Aelenei), imf@fct.unl.pt (I. Ferreira), maria.gloria.gomes@tecnico.ulisboa.pt (M.G. Gomes).

https://doi.org/10.1016/j.conbuildmat.2024.139309
Received 9 September 2024; Received in revised form 3 November 2024; Accepted 20 November 2024
Available online 22 November 2024

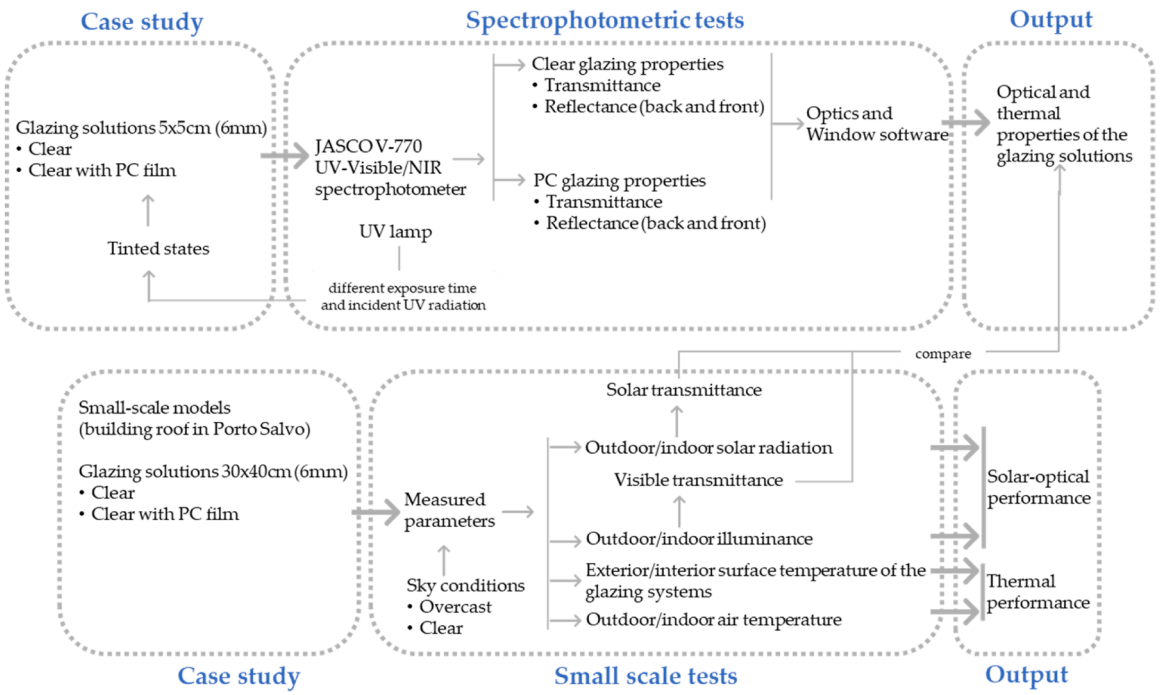

Fig. 1. Methodology scheme.

levels, maximizing solar heat gains during cold months and efficiently managing daylight to reduce artificial lighting energy use and promote thermal and visual comfort conditions [11].

Photochromic (PC) glazing [12], a type of passive smart glazing, can autonomously and reversibly alter its optical properties (chromatic change) in response to the intensity of solar radiation, mainly in the ultraviolet (UV) range, seeking to control solar heat gains and daylight transmission to promote comfort conditions and reduce energy use. This chromatic change occurs due to the incorporation of photosensitive crystals that appear colorless in the inactivated form and are generally embedded into host matrices (ceramic or polymers [13]) in a PC layer. When exposed to solar radiation, these crystals alter their molecule structure, shifting to a darker state; when the UV exposure diminishes, they return to a clear state [14]. Unlike active smart glazing systems that require electrical input, PC glazing operates passively, requiring no external energy source for its adaptive response [15].

While there is extensive research on the development of PC materials suitable for incorporation into building glazing [16,17], studies examining the in-situ performance of PC glazing systems on buildings remain scarce. Existing studies, primarily simulation-based [18–21], demonstrate the energy saving potential of PC glazing. A dynamic simulation of an office building by Cannavale et al. [18] resulted in energy savings with a PC glazing up to 20 % and on an increase of up to 20 % of useful illuminance levels, compared to clear glazing. Similarly, according to a dynamic simulation study conducted by Tällberg et al. [19], a PC glazing reduced up to 12 % the total energy use of an office room, compared to a clear glazing. Also considering a dynamic simulation model of an office room, Khaled & Berardi [20] observed higher energy savings (10–14 %) for entirely glazed South-oriented walls, against clear glazing, with more significant savings for desert and tropical climates. Considering the installation of PC glazing in a test-room, Nicoletti et al. [21] conducted an experimental and numerical test, achieving energy savings up to 9 % and improving useful illuminance up to 2 %, compared to clear glazing.

Despite these promising results, more empirical studies are needed to validate these simulation findings and deepen our understanding of the benefits of installing PC glazing on building façades. Therefore, this study's primary aim is to evaluate the thermal and solar-optical behavior of a PC film applied to single clear glazing under various sky conditions. The originality of this study lies in its experimental methodology, which involves small-scale and outdoor tests to monitor the real-time optical and thermal performance of a photochromic film. By evaluating the performance of this glazing solution in both overcast and clear sky conditions across different seasons, this research offers valuable insights into how this technology can adapt to varying solar intensities. Consequently, its findings contribute to the current knowledge on passive solar control strategies, demonstrating the effectiveness of photochromic glazing as a viable energy-saving technology in buildings. The findings can also be a valuable input for numerical studies, providing empirical data to validate or enhance simulation models for dynamic glazing technologies in building performance assessments.

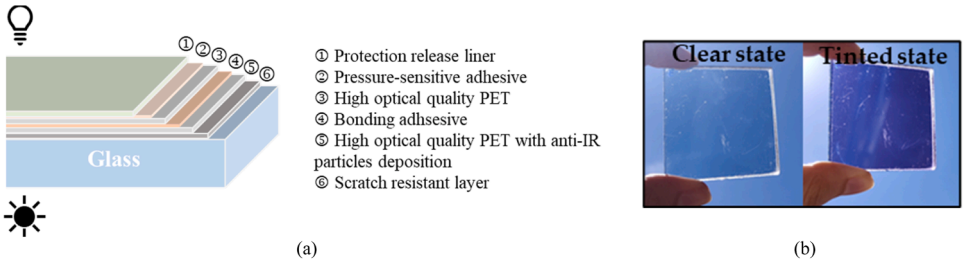

Fig. 2. Photochromic film: (a) material layers; (b) clear and tinted states, before and after exposure to solar radiation.

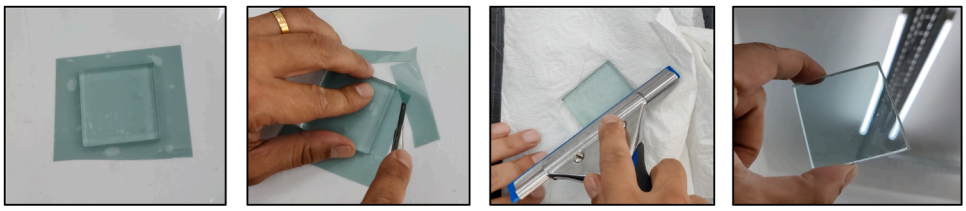

Fig. 3. Installation steps of the photochromic film: (a) placing the film on the wet glass substrate; (b) removing excessive film material; (c) eliminating bubbles; (d) air drying the filmed glazing.

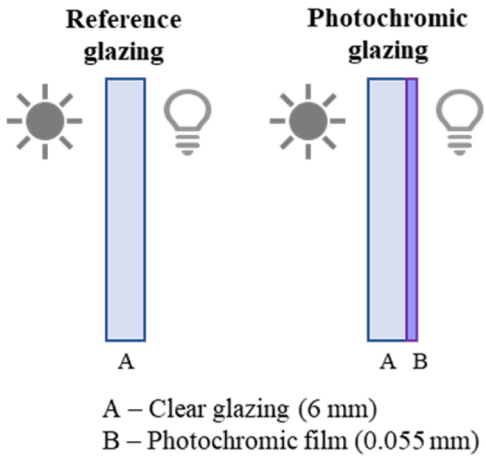

Fig. 4. Configuration of the analyzed glazing solutions.

2. Methods

The methodology adopted in the present study is shown in Fig. 1 and involves spectrophotometric tests and small-scale tests. The spectrophotometric tests were conducted to determine the optical properties of a PC film, varying the UV radiation intensity and exposure time. The small-scale tests were performed using two models to experimentally investigate the thermal and solar-optical behavior of the PC film, under real sky conditions (clear and overcast).

The PC film made of multiple material layers (Fig. 2a), manufactured with nanoceramic technology, has a thickness of 55μm, and tints in the presence of UV radiation (Fig. 2b) to provide shading according to the manufacturer. Even though there is no information about the durability of this PC film, the manufacturer offers a 2-year warranty. The behavior of this PC film, developed for installation on building façades, has also been assessed by the authors when installed on a double clear glazing system of an office room, in Lisbon [22].

For both laboratory and experimental tests, the PC film was installed on a clear single glazing (6 mm thickness), used as reference. To install the film, it was initially necessary to clean the glass substrate, spray it with water and place the film on the wet glass. Then, the excessive film material and the protection release liner were removed. Finally, the existing air and water bubbles were eliminated, and the film was left to completely dry. The installation steps for the glazing solution used in the spectrophotometric tests are illustrated in Fig. 3.

The configuration of the analyzed glazing solutions is shown in Fig. 4. Table 1 presents the optical and thermal properties of a clear single glazing (3 mm thick) with the PC film installed, provided in the film technical sheet [23]. The visible transmittance of the PC glazing varies between 20 % and 75 %, corresponding to the fully tinted and clear states, being significantly lower than the transmittance of conventional clear glazing. According to the information of the technical sheet other properties are not influenced by the presence of solar radiation. The transmittance of UV radiation through the PC glazing is extremely low (1 %), which can be beneficial for occupants' health and materials durability. These properties are presented as an initial characterization of the PC film before conducting the experimental tests. The properties of the glazing samples (6 mm thick) used in this study are presented in the results 3.1 after obtaining the transmittance and reflectance spectra.

2.1. Spectrophotometric tests

The spectral optical properties (transmittance and reflectance) of the two glazing solutions, using samples of 5x5cm, were measured through spectrophotometric tests.

An UV lamp (100 W), shown in Fig. 5a, with a spectral range of 370–430 nm was used to stimulate the PC film. Different exposure times (from 1 second to 5 minutes) and radiation levels were considered for the stimulation of the dynamic behavior of the PC film. The multiple radiation levels were achieved by varying the distance (0–80 cm with 10 cm intervals) between the lamp and the PC glazing sample. A CMP3 pyranometer from Kipp&Zonen [24], which has a flat spectral response between 300 and 2800 nm, was initially used to measure the radiation levels considering the distance variation (Fig. 5b). UV radiation levels between approximately 3 W/m^2 and 166 W/m^2 were obtain. The duration of the chromatic change of the PC glazing from tinted to clear state was also analyzed in the spectrophotometric tests.

The spectrophotometer JASCO V-770 UV-Visible/NIR [25] (Fig. 5c) featuring the 60 mm UV-Visible/NIR integrating sphere was used to measure the spectral transmittance and reflectance (front and back) of the glazing samples. This spectrophotometer measures wavelengths from 190 to 2700 nm, with an accuracy of ± 0.3 nm at 651.1 nm and ± 1.5 nm at 1312.2 nm. The spectroscopy software Spectra Manager™ Suite was used to operate the spectrophotometer. The glazing samples were carefully cleaned with a soft lint free cloth before conducting the experimental measurements. Depending on the property that is being measured (transmittance or reflectance), the placement of the glazing

Table 1
Thermal and optical properties of a clear single glazing (3 mm) with the photochromic film: thermal transmittance, U; solar factor, g; visible transmittance, τ_{vis}; visible front, ρ_{visF}, and back, ρ_{visB}, reflectance; solar transmittance, τ_{sol}; solar front, ρ_{solF}, and back, ρ_{solB}, reflectance; ultraviolet transmittance, τ_{UV}; absorptance of the glass pane, α.

	U [W/m^2 K)]	g [dimensionless]	τ_{vis} [%]	ρ_{visF} [%]	ρ_{visB} [%]	τ_{sol} [%]	ρ_{solF} [%]	ρ_{solB} [%]	τ_{UV} [%]	α [%]
Clear glazing + PC film (clear-tinted)	4.9	0.36	20–75	10	9	23	13	13	1	54

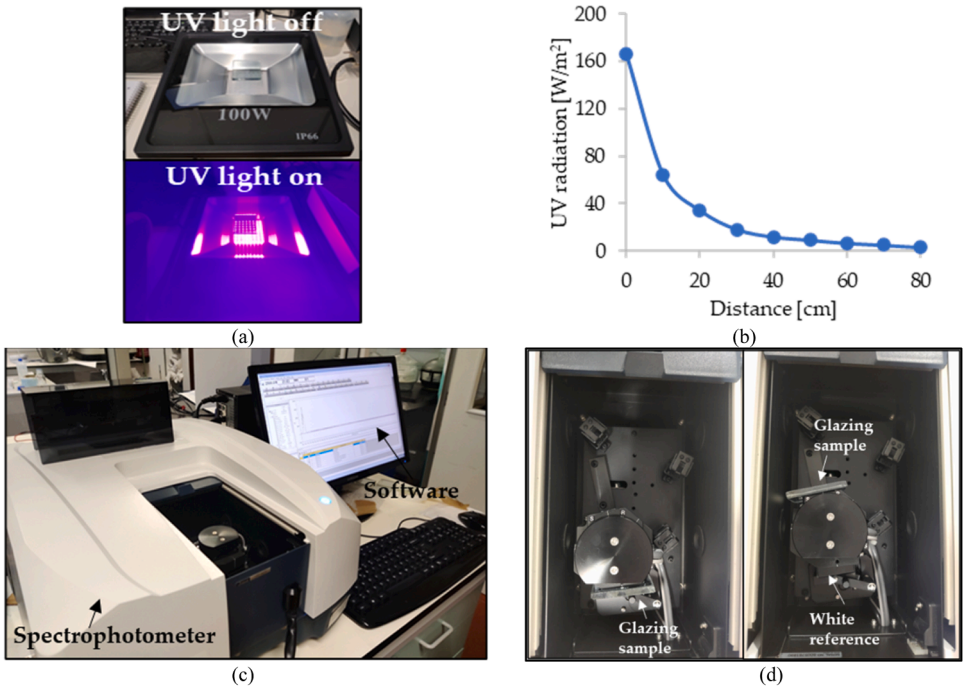

Fig. 5. Spectrophotometric testing: (a) UV lamp (off and on); (b) UV radiation incident on the PC glazing sample, in W/m^2, according to the distance from the lamp; (c) spectrophotometer JASCO V-770 and software; (d) placement of the glazing sample inside the integrating sphere for transmittance (left) and reflectance (right) measurements.

① TIR100-2 touch screen
② Black body half sphere (100°C when in use)
③ Measuring probe

Fig. 6. TIR100-2 used in the emissivity tests.

sample differed inside the integrating sphere as shown in Fig. 5d. The optical properties of the glazing solutions measured by the spectrophotometer are expected to help explaining the experimental results collected in the small-scale tests.

The thermal emissivity of the surfaces of both glazing samples was also measured using the instrument TIR100-2 [26] shown in Fig. 6. For the PC glazing, the emissivity tests were conducted with the film in the clear and tinted states.

2.2. Small-scale tests

The small-scale tests were conducted on the roof of Instituto Superior Técnico (Fig. 7a) at Taguspark campus, in Porto Salvo (Lisbon). Two small-scale models (Fig. 7b), with dimensions of 0.40 m (length) x 0.30 m (width) x 0.22 m (height), were constructed with black filmed marine plywood (0.02 m thickness). The models had small drill holes on the front and back surfaces to avoid the occurrence of extremely high temperature levels inside the models that could damage the experimental equipment. The black interior of the models made it possible to reduce the reflection of solar radiation by the internal surfaces, avoiding an overestimation of the experimental measurements by the

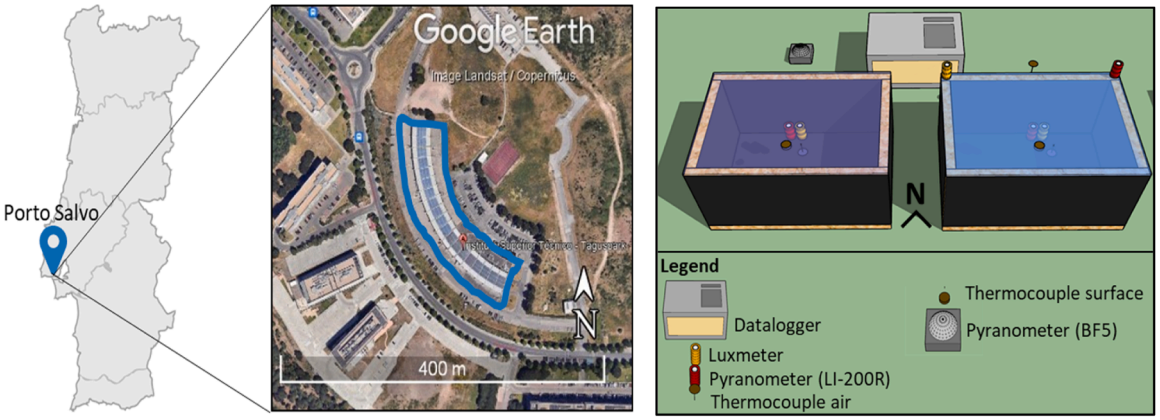

Fig. 7. Small-scale testing: (a) location of the building; (b) placement of the experimental equipment.

Table 2
Experimental equipment used in the small-scale tests and respective measured parameters.

Equipment	Manufacturer	Model	Accuracy	Parameter
Thermocouple		Type-T	± 0.2 °C at 100 °C	Indoor (T_{int}) and outdoor (T_{ext}) air temperature, interior ($T_{si,REF}$ and $T_{si,PC}$) and exterior ($T_{se,REF}$ and $T_{se,PC}$) surface glazing temperature
Pyranometer	Delta-T Devices	BF5	±20 W/m² ± 15 %	Outdoor global ($I_{ext,global}$) and diffuse ($I_{ext,diffuse}$) solar radiation in the horizontal plane
Pyranometer	LI-COR	LI−200R	±3 %	Outdoor (I_{ext}) and indoor ($I_{int,REF}$ and $I_{int,PC}$) solar radiation in the horizontal plane
Luxmeter	LI-COR	LI−210R	±5 %	Outdoor (E_{ext}) and indoor ($E_{int,REF}$ and $E_{int,PC}$) illuminance in the horizontal plane
Data logger	Delta-T Devices	DL2e	-	-

pyranometers and luxmeters. The analyzed glazing solutions were placed on top of each model.

The outdoor and indoor air temperature, along with the exterior and interior surface temperature of the glazing systems were measured using thermocouples. The outdoor (global and diffuse) and indoor (global) solar radiation, in the horizontal plane, was measured using pyranometers. The outdoor and indoor illuminance, in the horizontal plane, was measured using luxmeters. The experimental equipment was connected to a data logger that registered ten-minute averages from one-minute records. The placement of the experimental equipment is shown in Fig. 7b. The model, accuracy and measured parameter of each equipment is presented in Table 2. Parameters collected in the reference model are referred by REF and the ones collected in the photochromic model by PC.

The small-scale tests were conducted under overcast and clear sky conditions. A day with an overcast sky during winter season (when the occurrence probability of overcast sky conditions is higher) was selected, while two days with clear sky in different seasons (one during winter and another during summer) were selected to investigate the impact of incident solar radiation, solar altitude and outdoor air temperature on the performance of the glazing systems. The thermal behavior of the models was assessed through the outdoor/indoor air temperature and exterior/interior surface glazing temperature values. The luminous behavior was investigated through the measurements of outdoor/indoor solar radiation and illuminance levels. The solar (τ_{sol}) and visible (τ_{vis}) transmittance of each glazing was computed with the experimental data through Eqs. (1) and (2), respectively, and the obtained values were compared to the results of the spectrophotometric tests.

$$\tau_{sol} = \frac{E_{ext}}{E_{int}} \quad (1)$$

where E_{ext} and E_{int} are the exterior and interior solar radiation.

$$\tau_{vis} = \frac{I_{ext}}{I_{int}} \quad (2)$$

where I_{ext} and I_{int} are the exterior and interior illuminance.

3. Results

The results of the spectrophotometric tests and the small-scale tests are presented in Sections 3.1 and 3.2, respectively. The experimental results of the clear glazing are referred to as "REF", while the experimental results of the photochromic glazing are referred to as "PC".

3.1. Spectrophotometric tests

Fig. 8a illustrates the transmittance and reflectance (front and back) spectra of the REF glazing. High transmittance values were measured across the spectrum, as expected, with a mean value of 89 % between 400 and 2500 nm. The front and back reflectance spectra appear overlapped, with a mean value of 8 % between 400 and 2500 nm.

The transmittance and reflectance (front and back) spectra of the PC glazing in the totally clear and a tinted state are shown in Fig. 8b. The tinted state was achieved by exposing the PC glazing to the maximum incident UV radiation level (166 W/m² - Fig. 5) for 1 min. In both states, the PC glazing exhibits lower transmittance values across the spectrum compared to the REF glazing, mainly in the infrared range with a mean value of 13 %. In addition, contrary to the REF glazing, extremely low transmittance values in the UV range were measured with the PC glazing in both states. The highest transmittance value of the totally clear state (79 %) occurred at 490 nm. A significant change in the visible range of the transmittance spectra can be observed between the two states, with the tinted state exhibiting a minimum value (5 %) at 564 nm that is representative of a reduction of 95 % compared to the totally clear state.

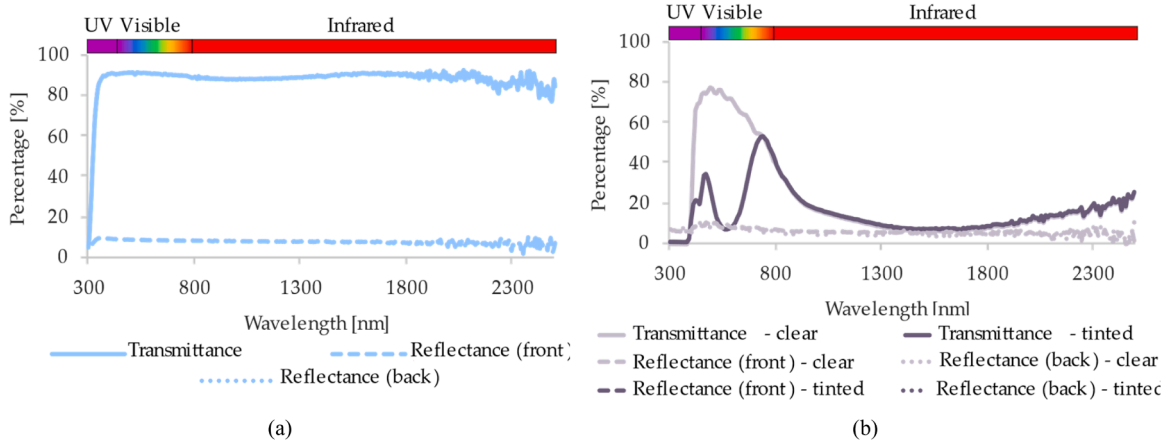

Fig. 8. Transmittance reflectance (front and back) spectra, from 300 to 2500 nm: (a) REF glazing; (b) PC glazing in the fully clear state and a tinted state (166 W/m² for 1 min).

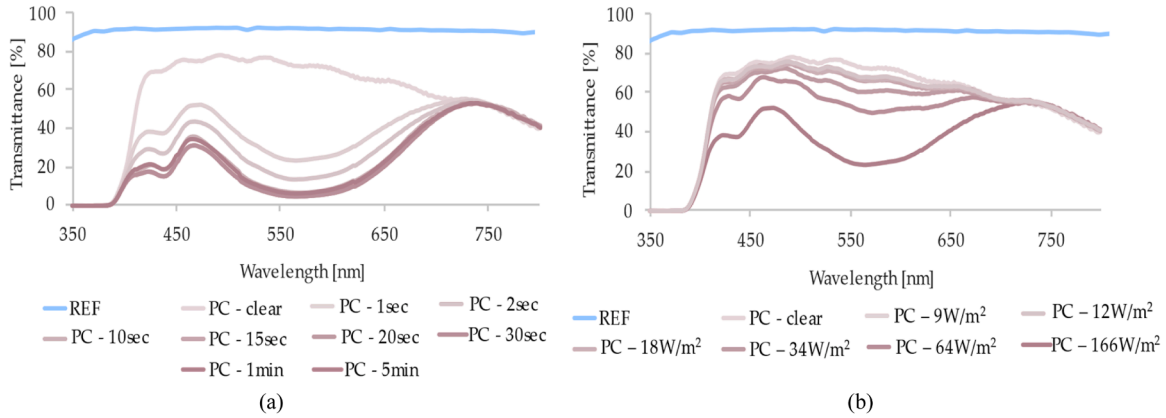

Fig. 9. Transmittance spectra, from 350 to 800 nm, of the PC glazing sample, along with the transmittance spectrum of the REF glazing: (a) different exposure times to the maximum UV radiation level; (b) 1-s exposure to different incident UV radiation levels.

Table 3
Thermal and optical properties of the analyzed single glazing solutions (clear without and with a photochromic film): thermal transmittance, U; solar factor, g; visible transmittance, τ_{vis}; visible front, ρ_{visF}, and back, ρ_{visB}, reflectance; solar transmittance, τ_{sol}; solar front, ρ_{solF}, and back, ρ_{solB}, reflectance; ultraviolet transmittance, τ_{UV}; absorptance of the glass pane, α.

Glazing solution	U [W/m² K)]	g [dimensionless]	τ_{vis} [%]	ρ_{visF} [%]	ρ_{visB} [%]	τ_{sol} [%]	ρ_{solF} [%]	ρ_{solB} [%]	τ_{UV} [%]	α [%]
Clear	5.81	0.87	91	9	9	90	8	8	60	8
Photochromic (clear-tinted)	5.81	0.57–0.44	73–11	8	8	40–21	6	6	0	54–73

The front and back reflectance spectra of the PC glazing are similar, appearing practically overlapped in Fig. 8b, and were not altered by the exposure to UV radiation. As a result, it is possible to state that the PC film reduces solar gains through the absorption mechanism.

As previously stated, to explore the impact of the incident UV radiation level and the exposure time on the dynamic behavior of the PC glazing, the sample was exposed to the multiple radiation levels presented in Fig. 5 for 1 s, 2 s, 10 s, 15 s, 30 s, 1 min and 5 min. The spectrophotometric measurements were taken for the wavelength range 350–800 nm since the dynamic behavior of the PC film is limited to the visible range (Fig. 8). This narrow wavelength range helps to avoid the reversing chromatic of the PC film during the spectrophotometer readings.

The transmittance spectra of the PC glazing exposed to the maximum UV radiation level for different exposure times, between 350 nm and 800 nm, are shown in Fig. 9a. As expected, longer exposure times corresponded to lower visible transmittance values. Apart from the 1 s and 2 s measurements, the spectra obtained for the different exposure times are very similar, practically overlapping, with the PC glazing quickly achieving a totally tinted state for this incident UV radiation level.

The transmittance spectra of the PC glazing exposed to multiple UV radiation levels for 1 s, between 350 nm and 800 nm, are shown in Fig. 9b. Higher incident UV radiation levels resulted in lower visible transmittance values. The spectra associated to UV radiation levels lower than 64 W/m^2 are similar, appearing overlapped for UV radiation levels equal and lower than 18 W/m^2.

The transmittance and reflectance spectra obtained for the REF glazing and the PC glazing in the totally clear and totally tinted states were used as input in Optics [27] and Window [28] software to compute the thermal and optical properties of the glazing solutions (Table 3). The installation of the PC film results in a decrease of the solar factor, visible and solar transmittance, and an increase of the solar absorptance, compared to the clear glazing without film.

With the transmittance results shown in Fig. 9a it is possible to note that after being exposed to the maximum UV radiation level for more than 10 seconds, the PC glazing achieved the tinted state, meaning that the chromatic change from clear to dark was very quick.

In order to investigate the duration of the chromatic change of the PC film from tinted to clear state, the spectrophotometer was used to measure the evolution of the absorbance of the glazing sample during 25 minutes after being exposed to the maximum UV radiation level for 5 minutes. The absorbance measurements were taken considering the wavelength of 500 nm, which is in the range of the dynamic behavior of the film. The visible transmittance (τ_{vis}) of the filmed glazing was then computed from the absorbance (A) measurements using Eq. (3). The temporal evolution of the visible transmittance of the PC glazing is shown in Fig. 10. It is possible to observe that the chromatic change occurs quickly in the first minutes, becoming slower after 10 minutes, finally reaching the clear state after 15 minutes (constant transmittance value → chromatic change ended).

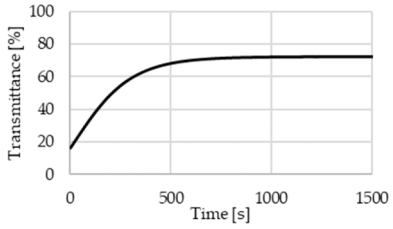

Fig. 10. Temporal evolution of the visible transmittance (at 500 nm) of the photochromic film (tinted to clear state).

$$\tau_{vis} = \text{antilog}(2 - A) \quad (3)$$

The thermal emissivity measured for the back and front surfaces of the two glazing samples is presented in Table 4. As expected from the results of the spectrophotometric tests, the presence of the PC film

Table 4
Thermal emissivity of the clear and photochromic glazing samples.

Clear glazing		Photochromic glazing			
		Front		Back	
Front	Back	Clear	Tinted	Clear	Tinted
0.84	0.84	0.84	0.84	0.89	0.89

Table 5
Average and maximum values of the outdoor solar radiation, illuminance and air temperature experimentally measured under overcast and clear sky.

Sky condition	$I_{ext,global}$ [W/m^2]		$I_{ext,diffuse}$ [W/m^2]		E_{ext} [klx]		T_{ext} [°C]	
	$\bar{x}$	M	$\bar{x}$	M	$\bar{x}$	M	$\bar{x}$	M
Overcast	178.7	482.9	160.6	328.6	21.2	54.4	14.5	17.2
Clear (winter)	505.1	781.3	44.5	54.6	49.0	76.4	20.1	25.5
Clear (summer)	722.9	1007.0	87.2	59.6	86.7	120.8	28.4	35.6

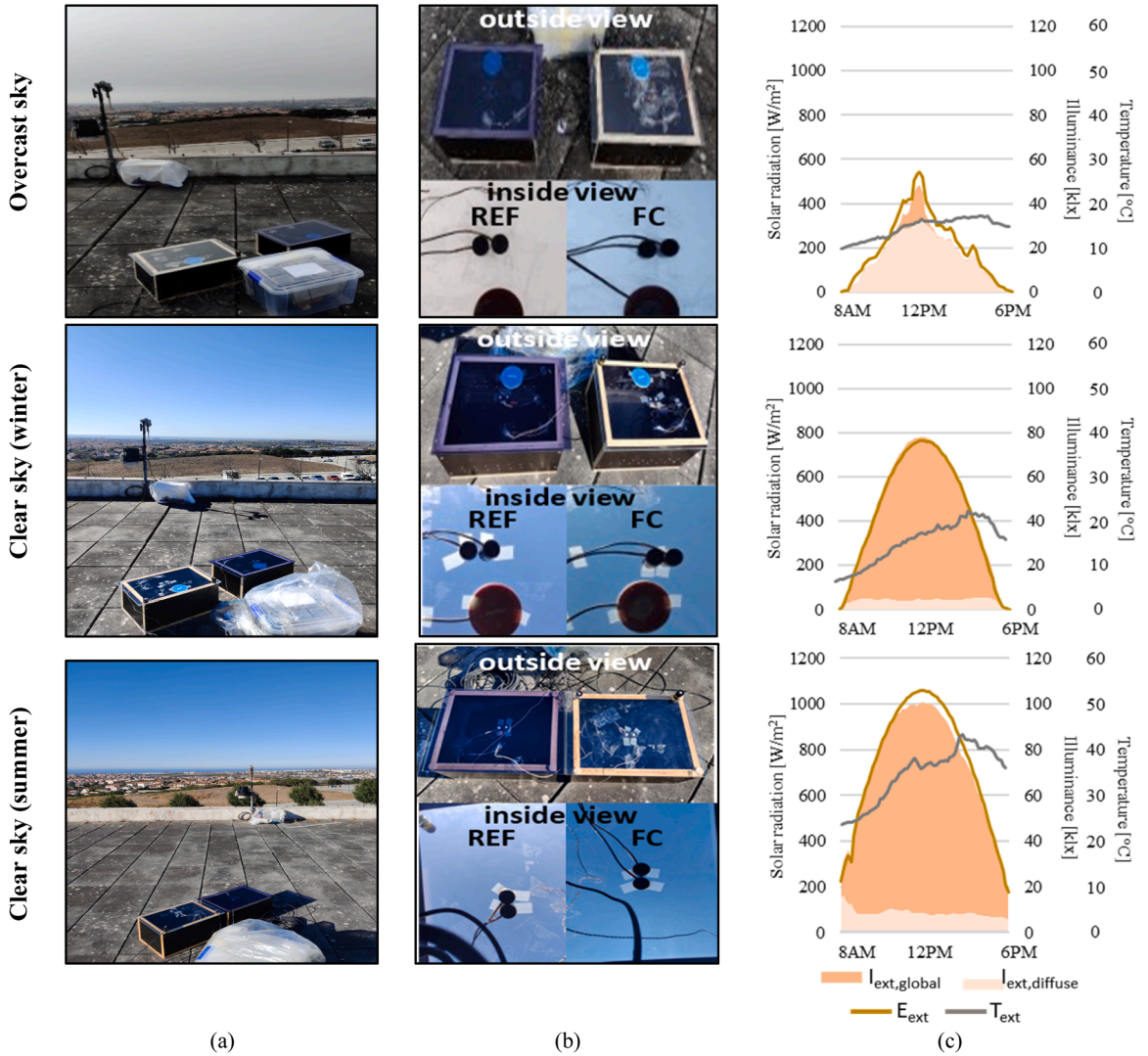

Fig. 11. (a) Photos with the sky condition, (b) outside and inside views of the small-scale models, (c) evolution of the outdoor global ($I_{ext,global}$) and diffuse ($I_{ext,diffuse}$) solar radiation, illuminance (E_{ext}) and air temperature (T_{ext}) measured during each day.

slightly increased the emissivity of the glazing surface it was applied to.

3.2. Small-scale tests

The outdoor solar radiation, illuminance and air temperature levels collected during the small-scale tests are shown in Table 5. The global solar radiation was significantly higher under clear sky, as expected, with significantly low diffuse solar radiation levels. The discrepancy in illuminance values between the two sky conditions is higher in terms of average values than maximum values. Both the average and maximum temperature values measured under clear sky were higher than the ones measured under overcast sky, particularly for the day with clear sky during summer.

Fig. 11a shows photos taken during the experimental tests, where it is possible to observe the sky conditions.

The outside and inside views of the small-scale models are shown in Fig. 11b, where it is possible to see that the PC glazing darkened (purple tone) under both sky conditions. The inside view of the PC glazing presents a blue tone. The evolution of the outdoor solar radiation, illuminance and air temperature measured during each day is shown in Fig. 11c. A peak of direct solar radiation occurred approximately at noon of the day with an overcast sky. The solar radiation was mainly direct during the days with clear sky, with diffuse solar radiation levels usually lower than 70 W/m^2. For the three days, the outdoor air temperature reached higher values during the afternoon.

3.2.1. Solar-optical behavior

The evolution of the outdoor and indoor solar radiation in each

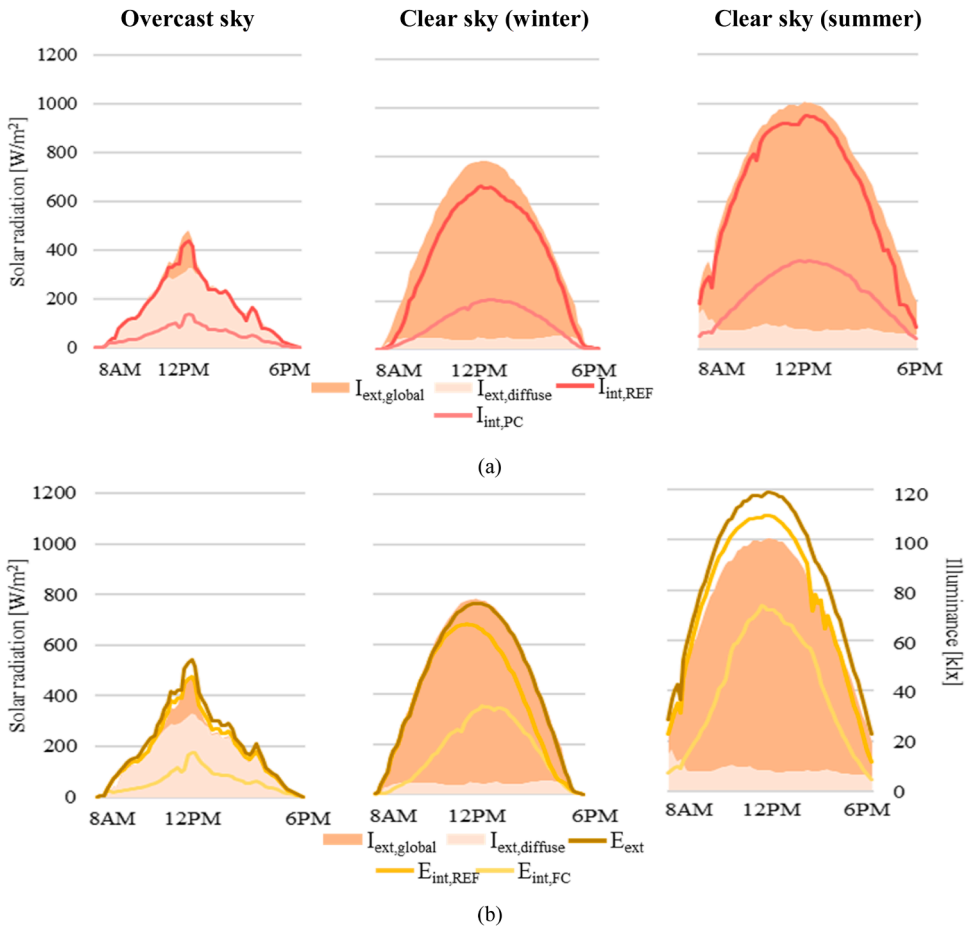

Fig. 12. Experimental results of the solar-optical behaviour, along with the outdoor global ($I_{ext,global}$) and diffuse ($I_{ext,diffuse}$) solar radiation, under overcast and clear sky conditions: (a) Evolution of the indoor solar radiation in each model ($I_{int,REF}$ e $I_{int,PC}$); (b) Evolution of the outdoor (E_{ext}) and indoor ($E_{int,REF}$ e $E_{int,PC}$) illuminance levels in each model.

model is shown in Fig. 12a. Under overcast sky conditions, the indoor solar radiation levels in the REF model were similar to the ones measured outside the model and significantly higher than the levels measured in the PC model. Under clear sky, the indoor solar radiation levels in the REF model were similar to the outdoor values only at the early morning and late afternoon periods. The PC glazing was effective on reducing the solar radiation levels inside the model, reaching peak values of 134.7 W/m^2 (overcast sky), 199.7 W/m^2 (clear sky in winter) and 360.6 W/m^2 (clear sky in summer), compared to the solar radiation levels in the REF model that reached peak values of 431.3 W/m^2 (overcast sky), 660.9 W/m^2 (clear sky in winter) and 951.5 W/m^2 (clear sky in summer).

Fig. 12b shows the evolution of the outdoor and indoor illuminance levels in each model, along with the outdoor solar radiation levels. The illuminance levels inside the REF model are slightly lower than the outdoor illuminance levels, in all days, with a larger discrepancy between values under clear sky conditions. The illuminance levels measured inside the PC model are significantly lower, under both sky conditions, reaching peak values of 18.3klx (overcast sky), 37.3klx (clear sky in winter) and 74.9klx (clear sky in summer), compared to the REF model that reached peak values of 48.0klx (overcast sky), 68.7klx (clear sky in winter) and 111.6klx (clear sky in summer). It is possible to observe a more significant reduction (between 60 % and 90 %) of the illuminance levels in the PC model during the morning period of the days with clear sky.

The solar and visible transmittance of each glazing system, shown in Fig. 13, were computed through the ratio between the solar radiation and illuminance levels measured outdoor and indoor in each model, as previously stated.

Fig. 13a shows the solar transmittance of each glazing system along with the outdoor solar radiation levels. Under overcast sky, the transmittance values obtained for the clear single glazing with and without film were mostly between 25 % and 35 % and 85–95 %, respectively. Under clear sky, the transmittance values are less stable during the day, which can be explained by an experimental error since multiple transmittance values were obtained for the clear single glazing that should present a static behavior (constant transmittance). The transmittance values obtained for the clear single glazing with and without film were mostly between 15 % and 35 % and 70 %-95 %, respectively, during the days with clear sky conditions. Comparing the results of the three days, lower solar transmittance values were obtained in the presence of the PC film, particularly under clear sky, which can be justified by the high solar radiation levels that promoted a more significant darkening of the film.

Fig. 13b shows the visible transmittance of each glazing system along with the outdoor solar radiation levels. Under overcast sky conditions, the visible transmittance values obtained for the clear single glazing with and without film were mostly between 20 % and 40 % and 85 %-95 %, respectively. Similar to what was observed in the solar transmittance results, the visible transmittance values are less stable under clear sky. Visible transmittance values between 10 % and 60 % and 60 %-95 % were obtained for the clear glazing with and without PC film, respectively, during the days with clear sky. Even though some of the visible transmittance values computed with clear sky are lower than the ones computed with overcast sky, some values are higher.

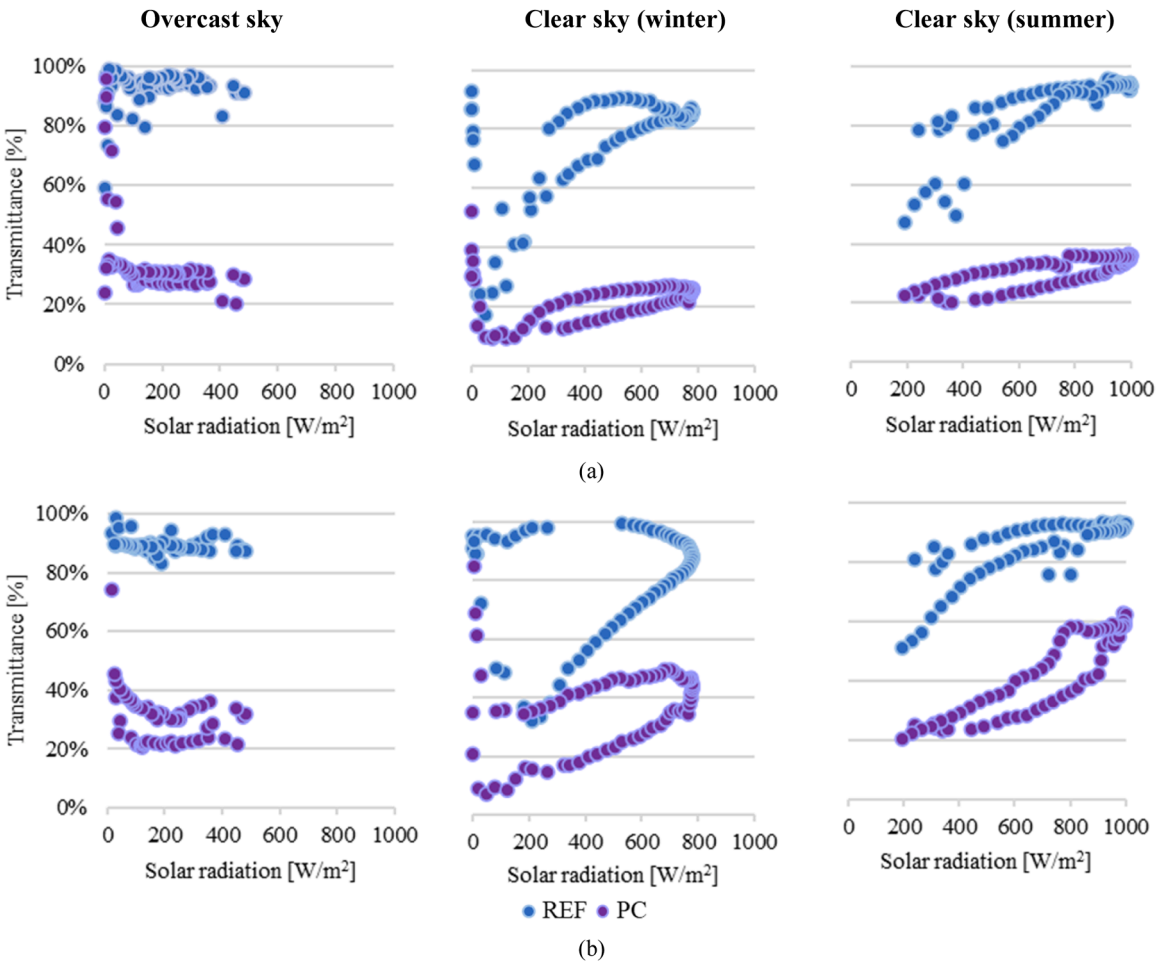

Fig. 13. Results of the solar (a) and visible (b) transmittance of each glazing system, along with the outdoor global solar radiation, under overcast and clear sky conditions.

3.2.2. *Thermal behavior*

The evolution of the outdoor air temperature and the exterior surface temperature of each glazing system in shown in Fig. 14a. The surface temperature of each glazing system was higher than the outdoor air temperature in both sky conditions, except during two short periods (in the early morning and late afternoon) during which the levels of solar radiation incident on the models were low. The peak values of the surface temperature of each glazing system matched the occurrence of the highest solar radiation levels, under overcast sky. Nevertheless, when assessing the measurements taken during the days with clear sky conditions, the peak values of the surface temperature of the glazing systems occurred during the afternoon, after the highest solar radiation levels. Despite the outdoor air temperature varying between the tested days, with higher temperature levels during the days with clear sky, it is possible to observe that the impact of the solar radiation levels in the performance of the glazing systems is more significant than the outdoor air temperature levels, for all days. Under both sky conditions, the surface temperature of the PC glazing system was always higher, reaching peak values of 31.4 °C (overcast sky), 39.0 °C (clear sky in winter) and 47.2 °C (clear sky in summer), compared to the REF glazing that reached peak values of 24.2 °C (overcast sky), 30.8 °C (clear sky in winter) and 41.7 °C (clear sky in summer). This discrepancy of surface temperature values can be explained by the solar absorptance of the PC film that promotes the increase of the temperature of the clear single glazing used as substrate.

Fig. 14b shows the evolution of the indoor air temperature in each model and the interior surface temperature of the glazing systems. The magnitude of the impact of the outdoor solar radiation levels on the models is confirmed by these results. The indoor air temperature of the REF model was always significantly higher than the surface temperature of the glazing, reaching peak values of 33.1 °C (overcast sky), 42.4 °C (clear sky in winter) and 60.9 °C (clear sky in summer). In contrast, the indoor air temperature of the PC model was lower than the interior surface temperature of the PC glazing during the morning and higher during the afternoon, for all days. This performance can be explained by the absorption of solar radiation by the PC film, which promotes the increase of the surface temperature and, consequently, the increase of the indoor temperature after some hours of exposure due to the reemission of radiation towards the indoor environment of the model. Nevertheless, the lower direct transmission of solar radiation made it possible to maintain the indoor air temperature of the PC model lower than the one measured in the REF model, being similar only during a period in the late afternoon with larger duration under clear sky conditions. The discrepancy between the surface temperature was more noticeable under clear sky conditions. The sharp increase of the indoor air temperature in the REF model during the morning period of the clear sky day in summer can be explained by the high incident solar radiation levels, coupled with the high solar transmittance of the glazing, that resulted in the increase of the black interior surfaces of the model and, consequently, in the increase of the indoor air temperature than the one observed in the PC model. The decrease of the indoor air temperature in the REF model in the afternoon period of the clear sky day in summer could result from natural air ventilation through the drill holes of the model due to potential wind.

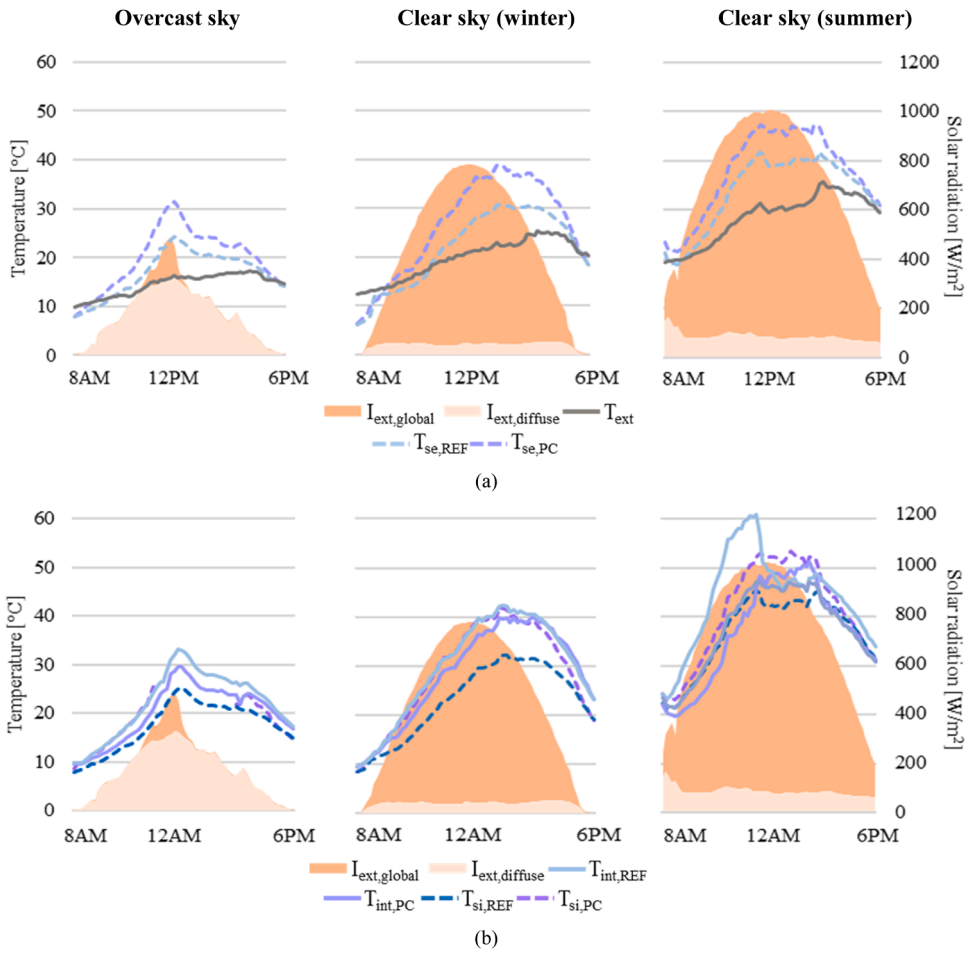

Fig. 14. Experimental results of the thermal behaviour, along with the outdoor global ($I_{ext,global}$) and diffuse ($I_{ext,diffuse}$) solar radiation, under overcast and clear sky conditions: (a) Evolution of the outdoor air temperature (Text) and exterior surface temperature of each glazing system ($T_{se,REF}$ and $T_{se,PC}$); (b) Evolution of the indoor air temperature in each model ($T_{int,REF}$ and $T_{int,PC}$) and of the interior surface temperature of each glazing system ($T_{si,REF}$ and $T_{si,PC}$).

4. Discussion

The added value of this study lies in the combination of spectrophotometric and small-scale tests that were developed to experimentally assess the performance of a photochromic (PC) glazing under artificial UV lighting and real sky conditions, including the computation of its optical properties. Because of the scarce scientific research on the topic, the findings resulting from this study regarding PC glazing performance are important and serve as baseline to more complex future studies.

According to the findings of this study, the PC glazing showed lower transmittance of solar radiation and illuminance levels, compared to clear glazing, under both sky conditions. Also, the increase of the solar absorptance of the PC glazing when tinted resulted in higher glazing surface temperature values, mainly of the interior surface temperature of the glazing system, compared to the clear glazing. Nevertheless, the indoor air temperature was lower in the presence of the PC glazing.

Regarding the thermal and optical properties of the PC glazing, the visible transmittance of the PC glazing computed with the spectrophotometric results is lower than the ones provided by the manufacturer, which can be explained by the larger thickness of the glazing used as substrate in this study but, mainly, by the fact that a high intensity UV lamp was used to stimulate the PC glazing. However, the solar and visible transmittance values of the PC glazing computed with the measurements of the spectrophotometric and the small-scale tests are in agreement.

Even though the spectrophotometric and small-scale tests conducted in this study made it possible to investigate the main optical properties of a PC glazing, against a clear glazing, and to explore its solar-optical and thermal behavior under real sky conditions, further studies including (but not limited to) full-scale experimental tests and simulation-based performance assessment are necessary for a better understanding of the installation potential of PC glazing. In addition, future work could also cover the performance of PC glazing against other passive and/or active smart glazing solutions.

5. Conclusions

The results of this study provide valuable insights into the spectrophotometric, solar-optical, and thermal performance of photochromic glazing to standard clear glazing. The main findings are as follows

Spectrophotometric Tests

- The back and front reflectance spectra of the PC glazing were similar and were not altered by the incidence of UV radiation, meaning the film blocks excessive solar heat gains through the absorption mechanism.
- The PC glazing exhibited a dynamic behavior in the visible range of the solar spectrum, with low transmittance values associated to higher incident UV radiation levels and longer exposure times. It is possible to state that the PC glazing can provide solar control even in its fully clear state due to its low transmittance in the near infrared range, compared to the clear glazing. Visible and solar transmittance values of 11 %-73 % and 21 %-40 %, respectively, were obtained for the PC film in the tinted-clear states.

Small-Scale Tests

- The PC glazing tinted under both overcast and clear sky conditions. The solar radiation levels transmitted through the PC glazing were significantly lower, under both sky conditions, with computed solar transmittance values between 25 % and 35 % (overcast sky) and 15 %-25 % (clear sky). The illuminance levels transmitted through the PC glazing were also significantly lower, with computed visible transmittance values between 20 % and 40 % (overcast sky) and 10 %-50 % (clear sky).
- The exterior and interior surface temperatures of the PC glazing increased. Nevertheless, a reduction of the indoor temperature, up to 14 %, was observed with the PC glazing under both sky conditions.

These findings demonstrate that PC glazing offers significant advantages in solar control, temperature regulation, and daylight management, making it a promising option for energy-efficient building applications.

CRediT authorship contribution statement

Henriqueta Teixeira: Writing – original draft, Methodology, Investigation. **Daniel Aelenei:** Writing – review & editing, Supervision, Methodology, Investigation. **A. Moret Rodrigues:** Writing – review & editing, Supervision, Methodology, Investigation. **M. Glória Gomes:** Writing – review & editing, Supervision, Methodology, Investigation, Conceptualization. **Isabel Ferreira:** Writing – review & editing, Methodology, Investigation.

Funding sources

The first author wishes to acknowledge the support of Fundação para a Ciência e a Tecnologia (FCT) for funding her Ph.D. Grant FCT PD/BD/150576/2020 (DOI: 10.5449/PD/BD/150576/2020). The authors thank FCT for funding the Civil Engineering Research and Innovation for Sustainability (CERIS) research unit through UIDB/04625/2020 (DOI: 10.54499/UIDB/04625/2020).

Declaration of Competing Interest

The authors declare that they have no known competing financial interests or personal relationships that could have appeared to influence the work reported in this paper.

Acknowledgements

The authors wish to express their gratitude to the IMPERSOL company for their technical support and to Clara Pacheco for her support during the experimental campaign. The authors extend their gratitude to the CERIS research unit of the Associação do Instituto Superior Técnico para a Investigação e Desenvolvimento.

Data availability

Data will be made available on request.

References

[1] W.J. Hee, M.A. Alghoul, B. Bakhtyar, O. Elayeb, M.A. Shameri, M.S. Alrubaih, K. Sopian, The role of window glazing on daylighting and energy saving in buildings, Renew. Sustain. Energy Rev. 42 (2015) 323–343, https://doi.org/10.1016/j.rser.2014.09.020.
[2] V.Ž. Leskovar, M. Premrov, Influence of glazing size on energy efficiency of timber-frame buildings, Constr. Build. Mater. 30 (2012) 92–99, https://doi.org/10.1016/j.conbuildmat.2011.11.020.
[3] G. Leftheriotis, P. Yianoulis, 3.10 - glazings and coatings, : Compr. Renew. Energy (2012) 313–355, https://doi.org/10.1016/B978-0-08-087872-0.00310-3.
[4] J. Pereira, H. Teixeira, M. da G. Gomes, A.M. Rodrigues, Performance of solar control films on building glazing: a literature review, Appl. Sci. (Switz.) 12 (2022) 5923, https://doi.org/10.3390/app12125923.
[5] J.L. Aguilar-Santana, H. Jarimi, M. Velasco-Carrasco, S. Riffat, Review on window-glazing technologies and future prospects, Int. J. Low -Carbon Technol. 15 (2019), https://doi.org/10.1093/ijlct/ctz032.
[6] H. Teixeira, M.G. Gomes, A. Moret Rodrigues, J. Pereira, Thermal and visual comfort, energy use and environmental performance of glazing systems with solar control films, Build. Environ. 168 (2020) 106474, https://doi.org/10.1016/J.BUILDENV.2019.106474.
[7] J. Pereira, M.G. Gomes, A.M. Rodrigues, M. Almeida, Thermal, luminous and energy performance of solar control films in single-glazed windows: use of energy performance criteria to support decision making, Energy Build. 198 (2019) 431–443, https://doi.org/10.1016/j.enbuild.2019.06.003.
[8] R.K. Jaysawal, S. Chakraborty, D. Elangovan, S. Padmanaban, Concept of net zero energy buildings (NZEB) - a literature review, Clean. Eng. Technol. 11 (2022) 100582, https://doi.org/10.1016/j.clet.2022.100582.
[9] S.D. Rezaei, S. Shannigrahi, S. Ramakrishna, A review of conventional, advanced, and smart glazing technologies and materials for improving indoor environment, Sol. Energy Mater. Sol. Cells 159 (2017) 26–51, https://doi.org/10.1016/j.solmat.2016.08.026.
[10] D. Li, Y. Wu, B. Wang, C. Liu, M. Arıcı, Optical and thermal performance of glazing units containing PCM in buildings: a review, Constr. Build. Mater. 233 (2020) 117327, https://doi.org/10.1016/j.conbuildmat.2019.117327.
[11] M. Boubekri, N. Boubekri, A review of the current state-of-the-art smart glazing and building skin materials designed to enhance daylighting design and reduce energy consumption in office buildings, J. Macro Trends Energy Sustain. 4 (2016) 47–58.
[12] A. Cannavale, Chromogenic technologies for energy saving, Clean. Technol. 2 (2020) 462–475, https://doi.org/10.3390/cleantechnol2040029.
[13] Y. Wang, E.L. Runnerstrom, D.J. Milliron, Switchable materials for smart windows, Annu Rev. Chem. Biomol. Eng. 7 (2016) 283–304, https://doi.org/10.1146/annurev-chembioeng-080615-034647.
[14] H. Miyazaki, T. Ishigaki, T. Ota, Photochromic smart windows employing WO3-based composite films, J. Mater. Sci. Res. 6 (2017) 62–66, https://doi.org/10.5539/jmsr.v6n4p62.
[15] Y. Ke, J. Chen, G. Lin, S. Wang, Y. Zhou, J. Yin, P.S. Lee, Y. Long, Smart windows: smart windows: electro-, thermo-, mechano-, photochromics, and beyond, Adv. Energy Mater. 9 (2019) 1902066, https://doi.org/10.1002/aenm.201970153.
[16] M. Hočevar, U. Opara Krašovec, A photochromic single glass pane, Sol. Energy Mater. Sol. Cells 186 (2018) 111–114, https://doi.org/10.1016/j.solmat.2018.06.035.
[17] L. Wang, Y. Liu, X. Zhan, D. Luo, X. Sun, Photochromic transparent wood for photo-switchable smart window applications, J. Mater. Chem. C. Mater. 7 (2019) 8649–8654, https://doi.org/10.1039/c9tc02076d.
[18] A. Cannavale, G. Zampini, F. Carlucci, M. Pugliese, F. Martellotta, U. Ayr, V. Maiorano, F. Ortica, F. Fiorito, L. Latterini, Energy and daylighting performance of building integrated spirooxazine photochromic films, Sol. Energy 242 (2022) 424–434, https://doi.org/10.1016/j.solener.2021.10.058.
[19] R. Tällberg, B.P. Jelle, R. Loonen, T. Gao, M. Hamdy, Comparison of the energy saving potential of adaptive and controllable smart windows: a state-of-the-art review and simulation studies of thermochromic, photochromic and electrochromic technologies, Sol. Energy Mater. Sol. Cells 200 (2019) 109828, https://doi.org/10.1016/j.solmat.2019.02.041.
[20] K. Khaled, U. Berardi, A cross-climate assessment of the visual and energy performance of flexible photochromic films for in-situ window retrofits, Energy Build. 300 (2023) 113664, https://doi.org/10.1016/j.enbuild.2023.113664.
[21] F. Nicoletti, D. Kaliakatsos, V. Ferraro, M.A. Cucumo, Analysis of the energy and visual performance of a building with photochromic windows for a location in southern Italy, Build. Environ. 224 (2022) 109570, https://doi.org/10.1016/j.buildenv.2022.109570.
[22] H. Teixeira, M.G. Gomes, A. Moret Rodrigues, D. Aelenei, Solar responsive building glazing: experimental analysis of the impact of photochromic glazing on indoor thermal and luminous conditions, J. Build. Eng. 92 (2024) 109812, https://doi.org/10.1016/j.jobe.2024.109812.
[23] Photochromic film Eclipse 40–80 C - Solar Screen, (n.d.). ⟨https://solarscreen.eu/en/products/eclipse-40-80-c⟩ (Accessed 12 May 2021).
[24] CMP3 spectrally flat Class C pyranometer - Kipp & Zonen, (n.d.). ⟨https://www.kippzonen.com/Product/11/CMP3-Pyranometer⟩ (Accessed 22 May 2024).
[25] V-770 UV–visible/NIR spectrophotometer | JASCO, (n.d.). ⟨https://jascoinc.com/products/spectroscopy/uv–visible-nir-spectrophotometers/models/v-770-uv–visible-nir-spectrophotometer/⟩ (accessed 18 November 2020).
[26] TIR100 – INGLAS, (n.d.). ⟨https://inglas.org/tir100/⟩ (Accessed 18 April 2024).
[27] Optics | Windows and Daylighting, (n.d.). ⟨https://windows.lbl.gov/software/optics⟩ (Accessed 24 January 2020).
[28] C. Curcija, S. Vidanovic, R. Hart, J. Jonsson, R. Mitchell, WINDOW Technical Documentation, Lawrence Berkeley Natl. Lab, 2018.